Published for SISSA by Springer

Received: October 9, 2013
Accepted: October 28, 2013
Published: November 14, 2013

NLO thermal dilepton rate at non-zero momentum

M. Laine

Institute for Theoretical Physics, Albert Einstein Center, University of Bern, Sidlerstrasse 5, CH-3012 Bern, Switzerland

E-mail: laine@itp.unibe.ch

Abstract: The vector channel spectral function and the dilepton production rate from a QCD plasma at a temperature above a few hundred MeV are evaluated up to next-to-leading order (NLO) including their dependence on a non-zero momentum with respect to the heat bath. The invariant mass of the virtual photon is taken to be in the range $\mathcal{K}^2 \sim (\pi T)^2 \sim (1\,\mathrm{GeV})^2$, generalizing previous NLO results valid for $\mathcal{K}^2 \gg (\pi T)^2$. In the opposite regime $0 < \mathcal{K}^2 \ll (\pi T)^2$ the loop expansion breaks down, but agrees nevertheless in order of magnitude with a previous result obtained through resummations. Ways to test the vector spectral function through comparisons with imaginary-time correlators measured on the lattice are discussed.

Keywords: Quark-Gluon Plasma, Thermal Field Theory, Lattice QCD

ArXiv ePrint: 1310.0164

doi:10.1007/JHEP11(2013)120

JHEP11(2013)120

Contents

JHEP11(2013)120

1 Introduction

Characteristics of "hard probes", produced within a thermal medium but immediately escaping it, are theoretically among the best ways to learn about the properties of the medium. For a plasma made of strongly interacting particles at a temperature of a few hundred MeV, which has a spatial extent of some tens of fm, typical hard probes are particles only experiencing weak and electromagnetic interactions, such as photons and leptons. Indeed the photon and dilepton production rates from a quark-gluon plasma have been studied in great detail in the last three decades (cf. e.g. refs. [1, 2]).

Even though hard probes behave as free particles once produced, their production mechanism is complicated, due to the strong interactions felt by the quarks and gluons that form the plasma. Therefore, despite the long history, our knowledge of the differential production rate as a function of temperature, baryon chemical potential, and quark mass spectrum, remains incomplete. In fact, in much of the parameter space, only the leading-order (LO) result in the strong coupling constant, α_s, is available. Given that α_s is not small at temperatures reached in practical heavy ion collision experiments, this could imply errors of up to 50% or so. It would be desirable to find ways to reduce the uncertainty,

and the current paper aims to play a role in this endeavour, by determining novel next-to-leading order (NLO) corrections to the production rate of a virtual photon subsequently decaying into a dilepton pair.

Denoting the four-momentum of the virtual photon, measured in the rest frame of the heat bath, by $\mathcal{K} = (k_0, \mathbf{k})$, with $k \equiv |\mathbf{k}|$ and $\mathcal{K}^2 \equiv k_0^2 - k^2$, the corresponding production rate (encoded in a *vector channel spectral function*) has been computed up to NLO, or $\mathcal{O}(\alpha_s)$, at $k = 0$ both for massless ($m \ll \pi T$) [3–5] and for heavy ($m \gg \pi T$) quarks [6]. At $k \neq 0$ only its asymptotics at $\mathcal{K}^2 \gg (\pi T)^2$ has been determined up to $\mathcal{O}(\alpha_s)$ [7]. The vacuum part of the vector spectral function is known up to N^{4}LO, or $\mathcal{O}(\alpha_s^4)$ [8, 9]. The goal of the present study is to complete the $\mathcal{O}(\alpha_s)$ level for a general $k \neq 0$, $T \neq 0$, with $\mathcal{K}^2 \sim (\pi T)^2$.

In contrast, for $0 < \mathcal{K}^2 \ll (\pi T)^2$, multiple scatterings take place within a typical formation time of the virtual photon. Consequently the loop expansion breaks down and needs to be resummed even to obtain the correct LO result. (The celebrated Hard Thermal Loop resummation [10] is not enough to render the loop expansion convergent on its own but a further all-orders resummation is needed, cf. ref. [11] for a recent discussion.) For the dilepton rate a resummation has been implemented both for $k \neq 0$ [12] (according to ref. [13] these results contain a slight error) and for $k = 0$ [14], following previous work on the production rate of on-shell photons [15–17]. Even though the current paper cannot serve as a crosscheck of these resummations, it is nevertheless comforting that a conceptually much simpler procedure yields qualitatively similar results as long as $\mathcal{K}^2$ is non-zero.

Of course, particularly for $0 < \mathcal{K}^2 \ll (\pi T)^2$, it may also be questioned whether the results are quantitatively accurate even if systematically resummed, because the effective value of α_s may be substantial. With this motivation in mind there have been attempts at lattice estimates of the vector channel spectral function. For quenched QCD, measurements of imaginary-time correlators are approaching the continuum limit both for $k = 0$ [18] and $k \neq 0$ [19]. Even though current extractions of the spectral functions may contain uncontrolled uncertainties [20], further progress will undoubtedly follow. Recent results also exist for dynamical quarks [21, 22], however in this case no continuum extrapolation has been carried out and systematic uncertainties are correspondingly larger. As will be discussed below a strict comparison of the perturbative and lattice results is not possible at present because of missing ingredients on both sides; nevertheless, on a semi-quantitative level a good agreement is found (for this it is essential that a continuum extrapolation has been carried out).

We start by outlining the ingredients of an NLO computation at $\mathcal{K}^2 \sim (\pi T)^2$ in section 2. The main results are given in section 3, together with comparisons with various limiting values. Numerical results for the vector channel spectral function and dilepton spectra are shown in section 4, whereas in section 5 the corresponding imaginary-time correlators, measurable with lattice simulations, are discussed. Section 6 offers a brief summary; two appendices collect various technical details related to the computation. (However the main computational ingredients, recently worked out in refs. [23, 24], will not be re-discussed here.)

JHEP11(2013)120

2 Setup

To leading order in $\alpha_e \equiv e^2/(4\pi)$ [25–27] and $\alpha_w \equiv g_w^2/(4\pi)$, the production rate of $\mu^-\mu^+$ (or e^-e^+) pairs from a hot QCD medium, with a total four-momentum $\mathcal{K}$, can be expressed as

$$\begin{aligned}
\frac{\mathrm{d}N_{\mu^-\mu^+}}{\mathrm{d}^4\mathcal{X}\mathrm{d}^4\mathcal{K}} &\overset{4m_\mu^2\ll\mathcal{K}^2\ll m_Z^2}{=} -\frac{n_{\mathrm{B}}(k_0)}{3\pi^3\mathcal{K}^2}\left(\eta_{\mu\nu}-\frac{\mathcal{K}_\mu\mathcal{K}_\nu}{\mathcal{K}^2}\right) \\
&\times\Bigg\{\alpha_e^2\left[\left(\sum_{i=1}^{N_{\mathrm{f}}}Q_i^2\right)\rho^{\mu\nu}_{\mathrm{V,NS}}(\mathcal{K})+\left(\sum_{i=1}^{N_{\mathrm{f}}}Q_i\right)^2\rho^{\mu\nu}_{\mathrm{V,SI}}(\mathcal{K})\right] \\
&+\frac{\alpha_e\alpha_w\mathcal{K}^2}{\mathcal{K}^2-m_Z^2}\frac{1-4s_w^2}{8(1-s_w^2)}\left[\left(\sum_{i=1}^{N_{\mathrm{f}}}Q_iC_{i,v}\right)\rho^{\mu\nu}_{\mathrm{V,NS}}(\mathcal{K})+\left(\sum_{i=1}^{N_{\mathrm{f}}}Q_i\right)\left(\sum_{i=1}^{N_{\mathrm{f}}}C_{i,v}\right)\rho^{\mu\nu}_{\mathrm{V,SI}}(\mathcal{K})\right] \\
&+\frac{\alpha_w^2\mathcal{K}^4}{(\mathcal{K}^2-m_Z^2)^2}\frac{1+(1-4s_w^2)^2}{256(1-s_w^2)^2}\Bigg[\left(\sum_{i=1}^{N_{\mathrm{f}}}C_{i,v}^2\right)\rho^{\mu\nu}_{\mathrm{V,NS}}(\mathcal{K})+\left(\sum_{i=1}^{N_{\mathrm{f}}}C_{i,v}\right)^2\rho^{\mu\nu}_{\mathrm{V,SI}}(\mathcal{K}) \\
&\qquad+\left(\sum_{i=1}^{N_{\mathrm{f}}}C_{i,a}^2\right)\rho^{\mu\nu}_{\mathrm{A,NS}}(\mathcal{K})+\left(\sum_{i=1}^{N_{\mathrm{f}}}C_{i,a}\right)^2\rho^{\mu\nu}_{\mathrm{A,SI}}(\mathcal{K})\Bigg]\Bigg\}\,,
\end{aligned} \tag{2.1}$$

where n_{B} is the Bose distribution, $s_w \equiv \sin\theta_w$ the weak mixing angle, $Q_i \in \left(\frac{2}{3},-\frac{1}{3}\right)$ the electric charge of quark of flavour i in units of e, and $C_{i,v} \in \left(1-\frac{8}{3}s_w^2,-1+\frac{4}{3}s_w^2\right)$, $C_{i,a}\in(-1,1)$ parametrise the vector and axial neutral-current couplings of up and down-type quark flavours, respectively. By $\rho^{\mu\nu}_{\mathrm{V,NS}}$ we denote the spectral function corresponding to the vector current in the "non-singlet" (NS) channel arising from quark-connected contractions; the "singlet" (SI) contributions arise instead from disconnected quark contractions. Flavour-degenerate quark masses have been assumed for the reduction in eq. (2.1). Setting the quark masses furthermore to zero, a Ward identity guarantees (in the absence of quark zero-mode contributions) that the non-singlet axial current spectral function ($\rho^{\mu\nu}_{\mathrm{A,NS}}$) agrees with the vector one. Moreover the singlet channels are suppressed by α_s^3 [9]. Therefore we concentrate on the non-singlet vector channel; because of current conservation it can be expressed as

$$\begin{aligned}
\rho_{\mathrm{NS}}(\mathcal{K}) &\equiv \left(\eta_{\mu\nu}-\frac{\mathcal{K}_\mu\mathcal{K}_\nu}{\mathcal{K}^2}\right)\rho^{\mu\nu}_{\mathrm{V,NS}}(\mathcal{K}) \\
&\equiv \int_{\mathcal{X}} e^{i\mathcal{K}\cdot\mathcal{X}}\left\langle\frac{1}{2}\left[\hat{\mathcal{J}}^\mu(\mathcal{X}),\hat{\mathcal{J}}_\mu(0)\right]\right\rangle_{\mathrm{c}}\,, \quad \hat{\mathcal{J}}^\mu\equiv\hat{\bar{\psi}}\gamma^\mu\hat{\psi}\,,
\end{aligned} \tag{2.2}$$

where c denotes a connected quark contraction.

The spectral function can be represented as an imaginary part of a retarded correlator which, in turn, is an analytic continuation of an imaginary-time (Euclidean) correlator:

$$\rho_{\mathrm{NS}}(\mathcal{K}) \;=\; \mathrm{Im}\,\Pi_{\mathrm{R}}(\mathcal{K}) \;=\; \mathrm{Im}\,\Pi_{\mathrm{E}}|_{k_n\to -i[k_0+i0^+]}\,. \tag{2.3}$$

The imaginary-time correlator is defined as

$$\Pi_{\mathrm{E}}(K)\equiv\int_0^{1/T}\mathrm{d}\tau\int_{\mathbf{x}}e^{iK\cdot X}\left\langle\left(\bar{\psi}\gamma^\mu\psi\right)(\tau,\mathbf{x})\,\left(\bar{\psi}\gamma_\mu\psi\right)(0,\mathbf{0})\right\rangle_T\,, \tag{2.4}$$

JHEP11(2013)120

where $K \equiv (k_n, \mathbf{k})$, with $k_n = 2\pi n T$, $n \in \mathbb{Z}$ denoting bosonic Matsubara frequencies; $K \cdot X = k_n \tau - \mathbf{k} \cdot \mathbf{x}$; and $\langle \ldots \rangle_T$ denoting a thermal expectation value. We first compute the imaginary-time correlator, and then determine the spectral function from eq. (2.3).

Before proceeding let us briefly elaborate on a more general case, with the imaginary-time correlator

$$\Pi_{\mathrm{E}}^{\mu\nu}(K) \equiv \int_0^{1/T} \mathrm{d}\tau \int_{\mathbf{x}} e^{iK\cdot X} \left\langle \left(\bar{\psi}\gamma^\mu \psi\right)(\tau, \mathbf{x}) \, \left(\bar{\psi}\gamma^\nu \psi\right)(0, \mathbf{0}) \right\rangle_T . \tag{2.5}$$

Because of current conservation all components are not independent; at finite temperature there are two independent structures. In terms of the spectral function, we can write

$$\mathrm{Im}\, \Pi_{\mathrm{R}}^{\mu\nu}(\mathcal{K}) \;=\; \mathbb{P}_{\mathrm{T}}^{\mu\nu}(\mathcal{K})\, \rho_{\mathrm{T}}(\mathcal{K}) + \mathbb{P}_{\mathrm{L}}^{\mu\nu}(\mathcal{K})\, \rho_{\mathrm{L}}(\mathcal{K}) \,, \tag{2.6}$$

where the projectors can be defined as

$$\mathbb{P}_{\mathrm{T}}^{\mu\nu}(\mathcal{K}) \;=\; -\eta^\mu{}_i \eta^\nu{}_j \left(\delta_{ij} - \frac{k_i k_j}{k^2}\right) = \eta^\mu{}_i \eta^\nu{}_j \left(\eta_{ij} + \frac{\mathcal{K}_i \mathcal{K}_j}{k^2}\right) , \tag{2.7}$$

$$\mathbb{P}_{\mathrm{L}}^{\mu\nu}(\mathcal{K}) \;=\; \eta^{\mu\nu} - \frac{\mathcal{K}^\mu \mathcal{K}^\nu}{\mathcal{K}^2} - \mathbb{P}_{\mathrm{T}}^{\mu\nu}(\mathcal{K}) \,. \tag{2.8}$$

Here the metric convention $\eta_{\mu\nu} \equiv \mathrm{diag}(+---)$ is assumed, and latin indices correspond to spatial directions. The mode labelled L is longitudinal with respect to the three-momentum $\mathbf{k}$; however, it is transverse with respect to $\mathcal{K}$. It is seen from eq. (2.2) that

$$\rho_{\mathrm{NS}}(\mathcal{K}) \;=\; \mathrm{Im}\, \Pi_{\mathrm{R}}(\mathcal{K}) \;=\; \left\{\mathrm{Im}\, \Pi_{\mathrm{R}}(\mathcal{K})\right\}^\mu{}_\mu \;=\; 2\rho_{\mathrm{T}}(\mathcal{K}) + \rho_{\mathrm{L}}(\mathcal{K}) \,, \tag{2.9}$$

and most of our discussion concerns this combination. However, in connection with lattice data in section 5 the two structures ρ_{T} and ρ_{L} are addressed separately.

The imaginary-time correlator of eq. (2.4) can be computed with regular path integral techniques. If evaluated perturbatively, its expression can be "scalarized", or reduced to a sum of a few independent "master" sum-integrals, all of which have an O(4) invariant appearance. Taking subsequently the cut defined in eq. (2.3), which removes terms independent of K, and choosing to work in dimensional regularization, with $D = 4 - 2\epsilon$ denoting the space-time dimension, the NLO expression reads

$$\begin{aligned}
\mathrm{Im}\, \Pi_{\mathrm{R}} = {} & 4(1-\epsilon) N_{\mathrm{c}}\, \rho_{\mathcal{J}_{\mathrm{b}}} \\
& + 8(1-\epsilon) g^2 N_{\mathrm{c}} C_{\mathrm{F}} \left\{ 2\left[\rho_{\mathcal{I}_{\mathrm{b}}} - \rho_{\bar{\mathcal{I}}_{\mathrm{b}}}\right] + 2(1-\epsilon)\left[\rho_{\mathcal{I}_{\mathrm{d}}} - \rho_{\bar{\mathcal{I}}_{\mathrm{d}}}\right] \right. \\
& \left. + 2\epsilon\, \rho_{\mathcal{I}_{\mathrm{f}}} - \frac{3+2\epsilon}{2}\, \rho_{\mathcal{I}_{\mathrm{g}}} + 2(1+\epsilon)\rho_{\mathcal{I}_{\mathrm{h}}} + 2(1-\epsilon)\rho_{\mathcal{I}_{\mathrm{h'}}} - \rho_{\mathcal{I}_{\mathrm{j}}} \right\} + \mathcal{O}\left(g^4\right) .
\end{aligned} \tag{2.10}$$

The coupling $g^2 \equiv 4\pi\alpha_s$ is the renormalized one, and $N_{\mathrm{c}} = 3$, $C_{\mathrm{F}} \equiv (N_{\mathrm{c}}^2 - 1)/(2N_{\mathrm{c}})$. Apart from all possible $2 \leftrightarrow 2$ scatterings, the NLO corrections incorporate $1 \leftrightarrow 3$ scatterings as well as virtual corrections to $1 \leftrightarrow 2$ scatterings [23]. The individual master spectral functions in eq. (2.10) stand for

$$\rho_{\mathcal{I}_{\mathrm{x}}} \equiv \mathrm{Im}[\mathcal{I}_{\mathrm{x}}]_{k_n \to -i[k_0 + i0^+]} \,, \tag{2.11}$$

JHEP11(2013)120

where the labelling refers to a notation employed in refs. [28, 29] (the definitions needed are repeated in appendix A). The statistics of the different propagators are identified by indices $\sigma_0, \ldots, \sigma_5$ as illustrated in eq. (A.11); more specifically, the two combinations appearing in eq. (2.10) carry the statistics

$$\rho_{\mathcal{I}_{\rm x}} \;\Leftrightarrow\; (\sigma_0\,\sigma_1\,\sigma_2\,\sigma_3\,\sigma_4\,\sigma_5) = (+----+)\;, \tag{2.12}$$

$$\rho_{\bar{\bar{\mathcal{I}}}_{\rm x}} \;\Leftrightarrow\; (\sigma_0\,\sigma_1\,\sigma_2\,\sigma_3\,\sigma_4\,\sigma_5) = (+--++-)\;. \tag{2.13}$$

Details concerning the evaluation of the different $\rho_{\mathcal{I}_{\rm x}}$'s can be found in refs. [23, 24].

Each of the master spectral functions can be written as

$$\rho_{\mathcal{I}_{\rm x}} = \rho^{\rm vac}_{\mathcal{I}_{\rm x}} + \rho^{T}_{\mathcal{I}_{\rm x}}\;, \tag{2.14}$$

where $\rho^{\rm vac}_{\mathcal{I}_{\rm x}}$ denotes a vacuum part. Only the vacuum parts have divergences at NLO; therefore, in coefficients multiplying the thermal parts, we can set $\epsilon \to 0$. The results obtained after these substitutions are given in the next section.

3 Main results

3.1 Strict NLO expression

Rewriting eq. (2.10) after the splitup in eq. (2.14), a subsequent expansion in ϵ up to $\mathcal{O}\left(\epsilon^0\right)$, and the insertion of known vacuum terms as listed in ref. [24] (the vacuum term of $\rho_{\mathcal{I}_{\rm j}}$ from ref. [23] vanishes), we get

$$\begin{aligned}\mathrm{Im}\,\Pi_{\rm R} = {} & -\frac{N_{\rm c} T \mathcal{K}^2}{2\pi k}\left\{1+\frac{3\alpha_s C_{\rm F}}{4\pi}\right\}\ln\left\{\frac{\cosh\left(\frac{k_+}{2T}\right)}{\cosh\left(\frac{k_-}{2T}\right)}\right\} \\ & + 32\pi\alpha_s N_{\rm c} C_{\rm F}\left\{2\left[\rho^T_{\mathcal{I}_{\rm b}} - \rho^T_{\bar{\bar{\mathcal{I}}}_{\rm b}} + \rho^T_{\mathcal{I}_{\rm d}} - \rho^T_{\bar{\bar{\mathcal{I}}}_{\rm d}}\right] - \frac{3}{2}\,\rho^T_{\mathcal{I}_{\rm g}} + 2\left[\rho^T_{\mathcal{I}_{\rm h}} + \rho^T_{\mathcal{I}_{\rm h'}}\right] - \rho^T_{\mathcal{I}_{\rm j}}\right\} + \mathcal{O}\left(\alpha_s^2\right).\end{aligned} \tag{3.1}$$

Here the light-cone momenta

$$k_\pm \equiv \frac{k_0 \pm k}{2} > 0 \tag{3.2}$$

have been defined. In addition we denote

$$M \equiv \sqrt{\mathcal{K}^2} > 0\;; \tag{3.3}$$

this "photon mass" is real in the time-like domain considered.

In figure 1, the LO and NLO results for $-\mathrm{Im}\,\Pi_{\rm R}/T^2$ are plotted as a function of M/T for various values of k/T. Only the time-like domain relevant for eq. (2.1) is shown. It can be observed that for $M \gtrsim \pi T$, any (Lorentz violating) dependence on the spatial momentum k/T is modest. For $M \ll \pi T$ the loop expansion breaks down because the NLO term overtakes the LO term. (This regime is discussed in more detail in section 3.3.)

JHEP11(2013)120

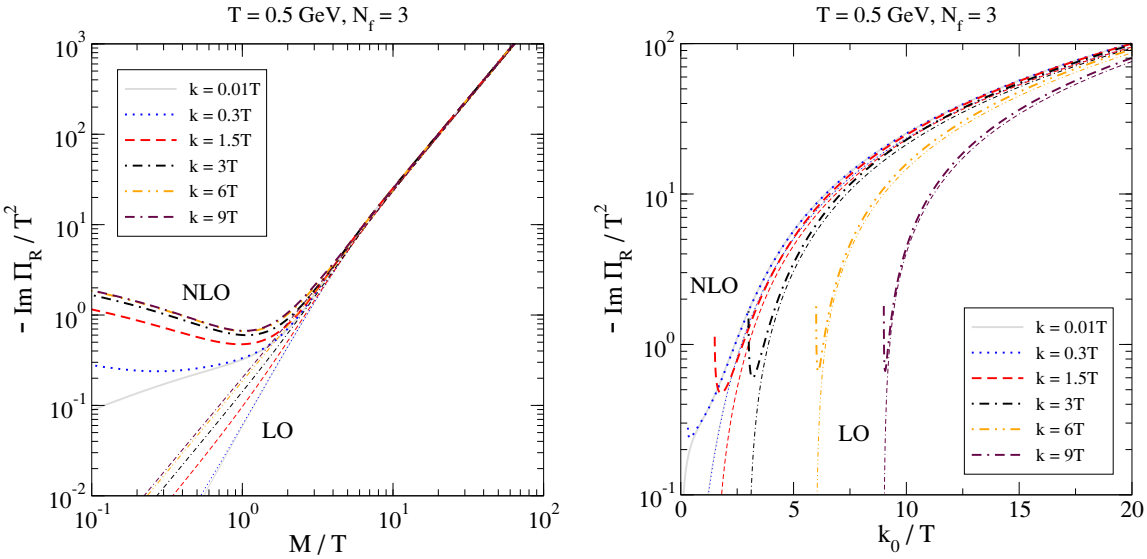

Figure 1. Strict loop expansion up to NLO. The same data is shown in two ways, as a function of M/T (left) and as a function of k_0/T (right), with $k_0 \geq \sqrt{k^2 + (0.1T)^2}$ in the latter case. The gauge coupling and the renormalization scale have been fixed as specified in appendix B ($\bar{\mu} = \bar{\mu}_{\rm ref}$ here).

3.2 Hard limit

The result of eq. (3.1) can be simplified in a "hard" limit $M \gg \pi T$, in which Operator Product Expansion (OPE) techniques become available [7]. In fact each of the master spectral functions can be expanded separately [30–32], displaying an expansion of the form

$$\rho_{\mathcal{I}_{\rm x}} \sim M^2 + T^2 + \frac{T^4}{M^2} + \mathcal{O}\left(\frac{T^6}{M^4}\right) . \tag{3.4}$$

When summed together, terms of $\mathcal{O}(T^2)$ cancel [7]. The remaining expression reads

$$-\mathrm{Im}\,\Pi_{\rm R} = \frac{N_{\rm c} M^2}{4\pi}\left\{1 + \frac{3\alpha_s C_{\rm F}}{4\pi}\right\} + \frac{16\alpha_s N_{\rm c} C_{\rm F}}{3}\,\frac{k_0^2 + k^2/3}{M^4}\int_p p(4n_{\rm F} - n_{\rm B}) + \mathcal{O}\left(\frac{\alpha_s T^6}{M^4}\right) , \tag{3.5}$$

where $n_{\rm F}$ is the Fermi distribution and

$$\int_p p\, n_{\rm B} = \frac{\pi^2 T^4}{30} , \qquad \int_p p\, n_{\rm F} = \frac{7\pi^2 T^4}{240} . \tag{3.6}$$

In figure 2 the expression from eq. (3.5) is compared with the full result from eq. (3.1). It is observed that the OPE results are accurate for $M \gtrsim 8T$. This is somewhat sooner than for generic individual NLO master spectral functions [23, 24]; the reason is that the LO result has only exponentially small thermal corrections for $M \gg \pi T$, so that large power corrections appearing in the full result are suppressed by $\mathcal{O}(\alpha_s)$.

3.3 Towards the soft limit

As is visible in figure 1, the NLO correction overtakes the LO term when $k_0 \to k^+$, and therefore the loop expansion breaks down. In this regime infinitely many loop orders

JHEP11(2013)120

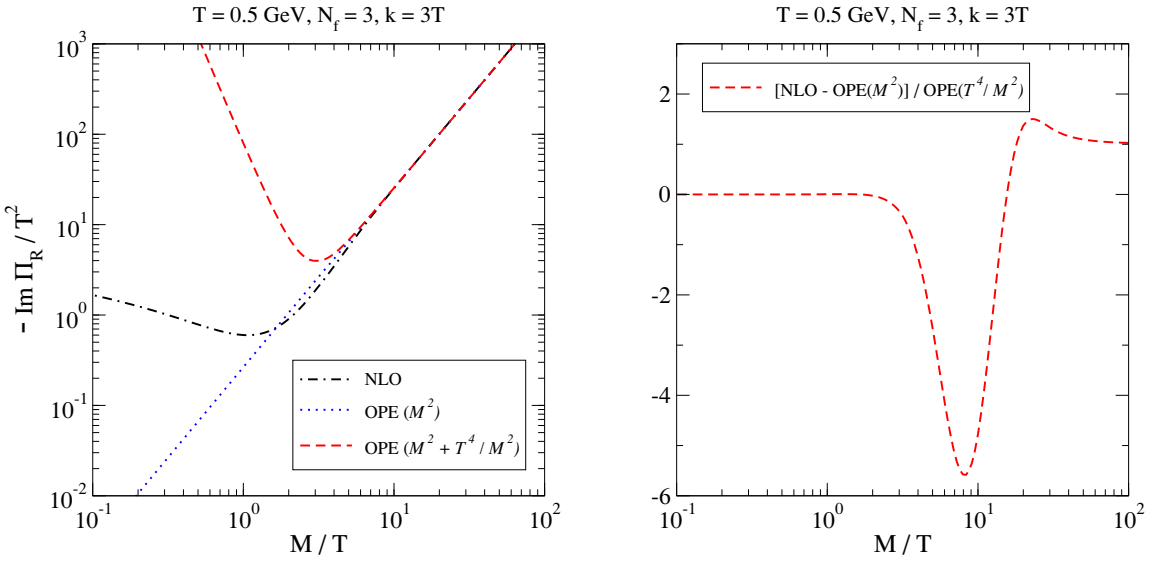

Figure 2. Left: comparison of the NLO result from eq. (3.1) at $k = 3T$ with the OPE formula from eq. (3.5), the latter evaluated up to various orders as indicated in the parentheses. Right: a relative difference probing the convergence of the expansion, with unity indicating that the $\mathcal{O}\left(T^4/M^2\right)$ correction dominates the remainder.

need to be resummed in order to obtain a consistent weak-coupling result. The technique goes under the name of the Landau-Pomeranchuk-Migdal (LPM) resummation (the Hard Thermal Loop (HTL) resummation is an ingredient but not sufficient on its own), and has been implemented for $k \sim \pi T$ in ref. [12] and for $k = 0$ in ref. [14]. The outcome cannot be expressed in analytic form, but requires a numerical solution of an inhomogeneous Schrödinger-type equation with a light-cone potential describing interactions.

Even though we do not discuss the soft regime $|k_0 - k| \ll \pi T$ systematically in the present paper, there are some qualitative remarks that can be made. Traditionally, one feature assigned to the soft regime is the generation of thermal masses to otherwise massless particles; in particular, for energetic quarks with $k \gtrsim \pi T$ the concept of an "asymptotic" thermal mass, denoted by

$$m_\infty^2 = \frac{g^2 C_{\rm F} T^2}{4} \,, \tag{3.7}$$

is assumed to be relevant [33]. Recomputing *naively* with the mass included, the LO result for the time-like domain reads [34] (this is often referred to as a thermal Drell-Yan process)

$$\mathrm{Im}\,\Pi_{\rm R}^{\rm LO,m_\infty} = -\frac{N_{\rm c}\left(M^2+2m_\infty^2\right)T}{2\pi k}\ln\left[\frac{\cosh\left(\frac{k_0+k\sqrt{1-4m_\infty^2/M^2}}{4T}\right)}{\cosh\left(\frac{k_0-k\sqrt{1-4m_\infty^2/M^2}}{4T}\right)}\right]\theta\left(k_0-\sqrt{k^2+4m_\infty^2}\right). \tag{3.8}$$

Now, if $m_\infty^2 \ll M^2$, as is the case in the regime in which our computation is valid, eq. (3.8)

JHEP11(2013)120

can be expanded to first non-trivial order in m_∞^2:

$$\mathrm{Im}\,\Pi_{\mathrm{R}}^{\mathrm{LO},m_\infty} = -\frac{N_{\mathrm{c}}\big(M^2+2m_\infty^2\big)\,T}{2\pi k}\ln\left\{\frac{\cosh\left(\frac{k_+}{2T}\right)}{\cosh\left(\frac{k_-}{2T}\right)}\right\} + \frac{N_{\mathrm{c}}m_\infty^2}{2\pi}\,[1-n_{\mathrm{F}}(k_+)-n_{\mathrm{F}}(k_-)] + \mathcal{O}\big(m_\infty^4\big)\,. \tag{3.9}$$

Remarkably, it can be verified that the $\mathcal{O}(m_\infty^2)$-terms here match *exactly* the contributions of the master spectral functions $\rho^T_{\mathcal{I}_{\mathrm{b}}}$, $\rho^T_{\tilde{\mathcal{I}}_{\mathrm{b}}}$, $\rho^T_{\mathcal{I}_{\mathrm{d}}}$ and $\rho^T_{\tilde{\mathcal{I}}_{\mathrm{d}}}$ in eq. (3.1), cf. eqs. (B.15) and (B.22) of ref. [24]. These master spectral functions are special in that they are the only ones containing a factorized thermal tadpole integral. Therefore, naive thermal mass resummation can be "topologically" justified through the NLO computation. In contrast, it does not have a power-counting justification: even though the factorized master spectral functions overtake the LO result at $M \ll \pi T$ (the LO result vanishes whereas these structures remain finite), these are not the dominant terms at $M \ll \pi T$, cf. figure 5.

The dominant master spectral function at $M \ll \pi T$ is the one denoted by $\rho^T_{\mathcal{I}_{\mathrm{h}}}$, (cf. eq. (A.9)), which diverges logarithmically in this limit:

$$\rho^T_{\mathcal{I}_{\mathrm{h}}}, \overset{M\ll\pi T}{\approx} -\frac{1}{32\pi}\ln\left(\frac{T^2}{M^2}\right)\Big[1-2n_{\mathrm{F}}(k)\Big]\int_p \frac{n_{\mathrm{B}}(p)+n_{\mathrm{F}}(p)}{p}\,, \tag{3.10}$$

where $\int_p n_{\mathrm{B}}/p = T^2/12$, $\int_p n_{\mathrm{F}}/p = T^2/24$. This well-known divergence [35] (the factor $-2n_{\mathrm{F}}(k)$ is often omitted) can be traced back to $2 \leftrightarrow 2$ scatterings with soft momentum exchange; the phase space distributions originate from the familiar structures [36] of gain and loss terms[1] of a Boltzmann equation [only quarks (q) and gluons (g) have phase space distributions; photons (γ) are not part of the medium]:

$$\begin{aligned}
&n_{\mathrm{F}}(k)\,n_{\mathrm{B}}(p)\,[1-n_{\mathrm{F}}(p)] - [1-n_{\mathrm{F}}(k)]\,[1+n_{\mathrm{B}}(p)]\,n_{\mathrm{F}}(p) && q(k)\,g(p) \leftrightarrow \gamma(k)\,q(p)\\
&+n_{\mathrm{F}}(k)\,n_{\mathrm{F}}(p)\,[1+n_{\mathrm{B}}(p)] - [1-n_{\mathrm{F}}(k)]\,[1-n_{\mathrm{F}}(p)]\,n_{\mathrm{B}}(p) && q(k)\,\bar{q}(p) \leftrightarrow \gamma(k)\,g(p)\\
&\quad = -\,[1-2n_{\mathrm{F}}(k)]\,[n_{\mathrm{B}}(p)+n_{\mathrm{F}}(p)]\,.
\end{aligned} \tag{3.11}$$

The divergence is lifted by Landau damping of the exchanged nearly-static quarks [37, 38] (cf. ref. [13] for an overview), an effect that becomes visible after an HTL resummation. In any case eq. (3.10) is not among the effects of simple mass resummation, eq. (3.9). (Even after the actual divergence has been lifted, the loop expansion still breaks down, because the NLO term overtakes the LO term for $M \lesssim gT$.)

To summarize, the most significant NLO corrections at $M \ll \pi T$ are not related to thermal mass generation, which has therefore *not* been implemented in the current study. They result rather from soft scatterings, and are as such a precursor to the enhancement over the LO result that has been found previously through more complete computations in this corner of the (k, k_0)-plane. A strength of the current "straightforward" analysis is that subtle issues of double-counting that have plagued resummed computations are avoided. Nevertheless, the current analysis breaks down at the latest when $\ln(\pi T/M) \gg 1$.

[1] The loss terms are eliminated if the additional factor $n_{\mathrm{B}}(k)$ from eq. (2.1) is multiplied in.

JHEP11(2013)120

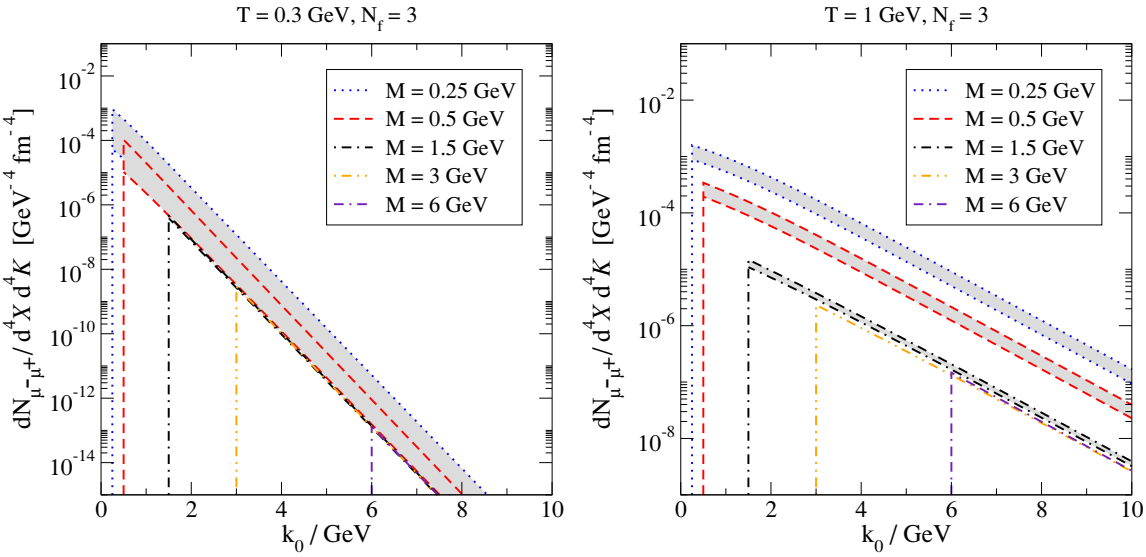

Figure 3. Thermal dilepton rates according to NLO perturbation theory, for $T = 0.3\,\mathrm{GeV}$ (left) and $T = 1\,\mathrm{GeV}$ (right), as a function of photon energy. The plots are for $N_\mathrm{f} = 3$ and $\Lambda_{\overline{\mathrm{MS}}} = 360\,\mathrm{MeV}$ [39]. Bands from scale variation are shown for the three smallest photon masses (cf. appendix B). The case $T = 1\,\mathrm{GeV}$ is shown in order to permit for a comparison with figure 7 of ref. [12]; the results are close except for an additional spike at the smallest k_0 for $M < 1.5\,\mathrm{GeV}$ in ref. [12]. (Peculiarly it appears that completely correct LO results for $M \ll \pi T$ have not been plotted in the literature [13].)

4 Dilepton spectra

We proceed to computing dilepton production spectra. Going over to physical units, *viz.*

$$\frac{\mathrm{d}N_{\mu^-\mu^+}}{\mathrm{d}^4\mathcal{X}\mathrm{d}^4\mathcal{K}} \times \mathrm{GeV}^4\mathrm{fm}^4 = \frac{\mathrm{d}N_{\mu^-\mu^+}}{\mathrm{d}^4\mathcal{X}\mathrm{d}^4\mathcal{K}} \left(\frac{1000}{197.327}\right)^4 , \tag{4.1}$$

results are shown for $N_\mathrm{f} = 3$, fixing $\Lambda_{\overline{\mathrm{MS}}} \simeq 360\,\mathrm{MeV}$ [39], in figure 3. The renormalization scale and its variation are chosen as specified in appendix B. Two temperatures are considered, and at each temperature results are plotted as a function of the photon energy k_0, for fixed values of the invariant photon mass M. For $T = 1\,\mathrm{GeV}$ a good overall agreement with the results of ref. [12] can be observed (on a logarithmic scale), despite the very different approximations inherent to the computations. For $M \gtrsim 1\,\mathrm{GeV}$ the results of the present study are more accurate than previous ones and, judging from the scale dependence, contain uncertainties on a 10–30 percent level.[2]

[2]The numerical results displayed in figure 3 can be downloaded from www.laine.itp.unibe.ch/dilepton-nlo/.

JHEP11(2013)120

5 Imaginary-time correlators

5.1 General considerations

The imaginary-time correlator corresponding to a spectral function ($\rho = \mathrm{Im}\,\Pi_{\mathrm{R}}$) antisymmetric in $k_0 \to -k_0$ is given by

$$G_{\mathrm{E}}(\tau) = \int_0^\infty \frac{\mathrm{d}k_0}{\pi}\, \mathrm{Im}\,\Pi_{\mathrm{R}}(k_0,\mathbf{k}) \frac{\cosh\left(\frac{1}{2T}-\tau\right)k_0}{\sinh\left(\frac{k_0}{2T}\right)} \,. \tag{5.1}$$

A powerlike growth of $\mathrm{Im}\,\Pi_{\mathrm{R}}$ at $k_0 \gg \pi T$ leads to a powerlike divergence of $G_{\mathrm{E}}(\tau)$ at $\tau \ll 1/T$; this divergence should be subtracted from numerical data [40] in order for a well-defined analytic continuation to be possible at least in principle [41]. The power divergence is determined by employing a vacuum spectral function in eq. (5.1). In the following we start by working out "reference" imaginary-time correlators which contain a vacuum-like spectral function modified by LO thermal corrections (section 5.2); subsequently issues related to NLO and higher thermal modifications are commented upon (section 5.3).

According to eq. (2.6) the vector spectral function contains two independent parts. In this paper, we have computed the contraction $\mathrm{Im}\,\{\Pi_{\mathrm{R}}\}^{\mu}{}_{\mu} = 2\rho_{\mathrm{T}} + \rho_{\mathrm{L}}$ up to NLO in the time-like domain $k_0 \geq k$, cf. eq. (2.9). There are two separate challenges which prohibit a direct comparison with the continuum-extrapolated lattice measurements reported in ref. [19]:

(i) According to eq. (5.1) the space-like domain $k_0 < k$ contributes to $G_{\mathrm{E}}(\tau)$, even though it plays no role for the dilepton rate, which includes a prefactor $\theta(\mathcal{K}^2 - 4m_\mu^2)$ for a finite muon mass. *The space-like domain was not worked out in the present paper at NLO.*

(ii) In ref. [19] the momentum was chosen as $\mathbf{k} = (k,0,0)$ and the components G_{11} and $G_{22} = G_{33}$ of the vector correlator were analyzed. It can be deduced from eqs. (2.6)–(2.8) that these correlators are determined by the spectral functions $\{\mathrm{Im}\,\Pi_{\mathrm{R}}\}_{11} = -k_0^2\,\rho_{\mathrm{L}}/\mathcal{K}^2$ and $\{\mathrm{Im}\,\Pi_{\mathrm{R}}\}_{22} = \{\mathrm{Im}\,\Pi_{\mathrm{R}}\}_{33} = -\rho_{\mathrm{T}}$, respectively (for the time component, $\{\mathrm{Im}\,\Pi_{\mathrm{R}}\}_{00} = -k^2\,\rho_{\mathrm{L}}/\mathcal{K}^2$). Unfortunately knowledge of G_{11} in configuration space does not allow us to extract G_{00}, because the Ward identity

$$\partial_\tau^2 G_{00}(\tau) = k^2 G_{11}(\tau)\,, \qquad 0 < \tau < \frac{1}{T}\,, \tag{5.2}$$

does not have a unique solution. *Due to a missing G_{00} the results of ref. [19] are not sufficient for extracting the full vector correlator $G_{00} - G_{ii}$.*

To rectify the second problem, all that is needed is an estimate of G_{00}, which is presumably simply a matter of analyzing existing data. To overcome the first problem, a dedicated study of the domain $k_0 < k$ is needed. In the next section we do consider $k_0 < k$ at LO, but NLO corrections are left to future work.

JHEP11(2013)120

5.2 Contribution from hard physics

In order to estimate the imaginary-time correlators G_{11} and $G_{22} = G_{33}$ measured in ref. [19], information is needed about the two spectral functions $\rho_{\rm T}$, $\rho_{\rm L}$ appearing in eq. (2.6). These are more complicated than the sum $2\rho_{\rm T} + \rho_{\rm L}$; for instance, at LO,

$$\rho_{\rm T}^{\rm LO} = -\frac{2N_{\rm c}\mathcal{K}^2}{k^2}\left[\frac{k_0^2+k^2}{2}\langle 1\rangle - 2\big\langle p(k_0-p)\big\rangle\right] , \tag{5.3}$$

$$\rho_{\rm L}^{\rm LO} = +\frac{4N_{\rm c}\mathcal{K}^2}{k^2}\left[\frac{k_0^2-k^2}{2}\langle 1\rangle - 2\big\langle p(k_0-p)\big\rangle\right] , \tag{5.4}$$

where

$$\langle \ldots\rangle \equiv \frac{1}{16\pi k}\left\{\theta(k_-)\int_{k_-}^{k_+}{\rm d}p \, - 2\theta(-k_-)\int_{k_+}^{\infty}{\rm d}p\right\}\left[n_{\rm F}(p-k_0) - n_{\rm F}(p)\right](\ldots) . \tag{5.5}$$

For $k_+ > 0$ but k_- of either sign, the values of the moments read (cf. ref. [34])

$$\langle 1\rangle = \frac{1}{\pi k}\left\{\frac{T}{8}\ln\left(\frac{1+e^{-k_+/T}}{1+e^{-|k_-|/T}}\right) + \frac{\theta(k_-)\,k}{16}\right\} , \tag{5.6}$$

$$\begin{aligned}\big\langle p(k_0-p)\big\rangle = \frac{1}{\pi k}\Bigg\{ & \frac{\mathcal{K}^2 T}{32}\ln\left(\frac{1+e^{-k_+/T}}{1+e^{-|k_-|/T}}\right) + \frac{\theta(k_-)\,k\left(3k_0^2-k^2\right)}{192} \\ & + \frac{kT^2}{8}\left[{\rm Li}_2\left(-e^{-k_+/T}\right) + {\rm sign}(k_-)\,{\rm Li}_2\left(-e^{-|k_-|/T}\right)\right] \\ & + \frac{T^3}{4}\left[{\rm Li}_3\left(-e^{-k_+/T}\right) - {\rm Li}_3\left(-e^{-|k_-|/T}\right)\right]\Bigg\} .\end{aligned} \tag{5.7}$$

As is readily visible from eqs. (5.3), (5.4), the complicated $\langle p(k_0-p)\rangle$ drops out in eq. (2.9):

$$\left\{{\rm Im}\,\Pi_{\rm R}^{\rm LO}\right\}^{\mu}{}_{\mu} = 2\rho_{\rm T}^{\rm LO} + \rho_{\rm L}^{\rm LO} = -4N_{\rm c}\,\mathcal{K}^2\langle 1\rangle . \tag{5.8}$$

This simplification is analogous to that enjoyed by the bulk channel spectral function, extracted from a vacuum-like Lorentz structure [28], as compared with the shear channel one, in which a larger class of structures containing spatial momenta appears [29].

Consider now the limit $k_+, |k_-| \gg \pi T$. Then many terms drop out from eqs. (5.6), (5.7) and the spectral functions become

$$\rho_{\rm T}^{\rm LO}\,, \rho_{\rm L}^{\rm LO} \overset{k_+,|k_-|\gg\pi T}{\approx} -\frac{N_{\rm c}\mathcal{K}^2\,\theta\left(\mathcal{K}^2\right)}{12\pi} , \tag{5.9}$$

so that

$${\rm Im}\left\{\Pi_{\rm R}^{\rm LO}\right\}_{\mu\nu} \overset{k_+,|k_-|\gg\pi T}{\approx} \left(\eta_{\mu\nu} - \frac{\mathcal{K}_\mu\mathcal{K}_\nu}{\mathcal{K}^2}\right)\left(-\frac{N_{\rm c}\mathcal{K}^2}{12\pi}\right)\theta\left(\mathcal{K}^2\right) . \tag{5.10}$$

This is simply a vacuum result. In vacuum, the spectral function is known up to 5-loop level [8, 9]. In the following we take the LO thermal $\rho_{\rm T}$, $\rho_{\rm L}$ and multiply them by the same *vacuum* factor; the results are loop-level correct for $|\mathcal{K}^2| \gg (\pi T)^2$ and LO correct at $|\mathcal{K}^2| \sim (\pi T)^2$ but in general underestimate thermal corrections.

JHEP11(2013)120

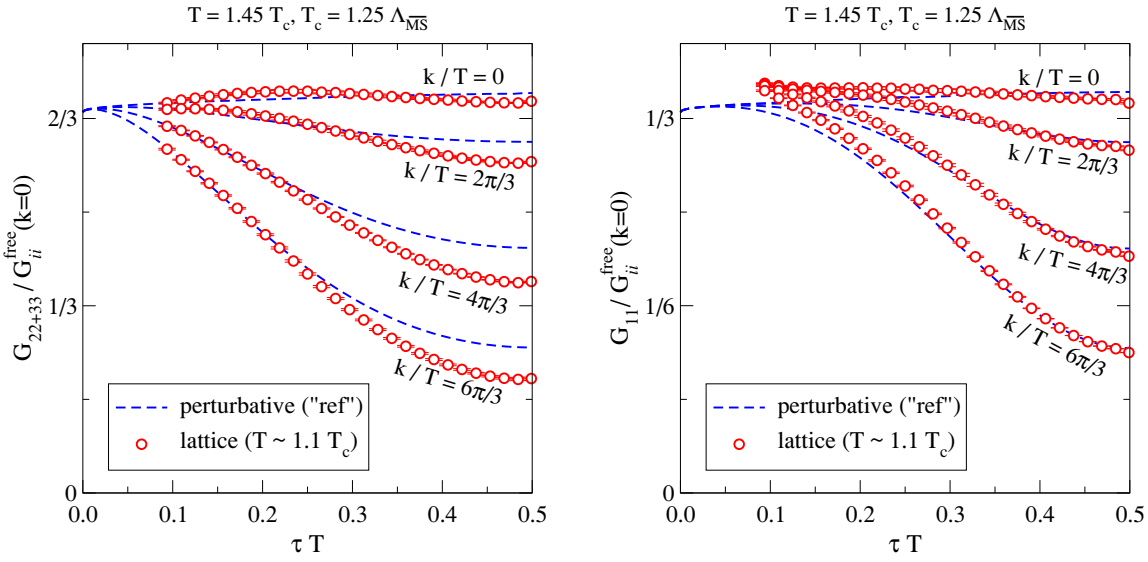

Figure 4. Imaginary-time correlators based on eq. (5.12), normalized to eq. (5.13), for $N_{\rm f} = 0$. The perturbative values are compared with lattice data from ref. [19] (to make use of the data a continuum value of the quark-number susceptibility is needed; we have assumed $\chi_{\rm q} \simeq 0.88T^2$). The data are for $T = 1.1T_{\rm c}$ but according to ref. [19] they are close to those at $T = 1.45T_{\rm c}$ where the perturbative expressions were evaluated. Note that for $k = 0$, $G_{22+33} = 2G_{11}$, and the violation of this relation towards small τT is a reflection of systematic uncertainties related to the continuum extrapolation.

Denoting $\ell \equiv \ln\left(\bar{\mu}^2/\mathcal{K}^2\right)$, the vacuum factor [8] can be expressed as

$$\mathcal{R}(\mathcal{K}^2) \equiv \theta\left(\mathcal{K}^2\right) \mathrm{sign}(k_0) \Big\{ r_{0,0} + r_{1,0}\, a_s + \left(r_{2,0} + r_{2,1}\,\ell\right)\, a_s^2 + \left(r_{3,0} + r_{3,1}\,\ell + r_{3,2}\,\ell^2\right)\, a_s^3 + \left(r_{4,0} + r_{4,1}\,\ell + r_{4,2}\,\ell^2 + r_{4,3}\,\ell^3\right)\, a_s^4 + \mathcal{O}\left(a_s^5\right) \Big\}, \tag{5.11}$$

where $a_s \equiv \alpha_s/\pi$ and the coefficients are identical to those listed in ref. [20] (the terms $r_{0,0} + r_{1,0}\, a_s$ reproduce the factor $1 + \frac{3\alpha_s C_{\rm F}}{4\pi}$ from eq. (3.5)). We set

$$\rho_{\rm T}^{\rm ref} \equiv \rho_{\rm T}^{\rm LO}\, \mathcal{R}\left(\max\left\{\mathcal{K}^2, (\pi T)^2\right\}\right)\,, \qquad \rho_{\rm L}^{\rm ref} \equiv \rho_{\rm L}^{\rm LO}\, \mathcal{R}\left(\max\left\{\mathcal{K}^2, (\pi T)^2\right\}\right)\,, \tag{5.12}$$

freezing the $\mathcal{R}$-factor when entering the thermal domain. The renormalization scale is fixed as specified in appendix B. The results are normalized to the free correlator for $k = 0$ [42],

$$G_{ii,k=0}^{\rm free}(\tau) \equiv 6T^3 \left[\pi(1-2\tau T)\frac{1+\cos^2(2\pi\tau T)}{\sin^3(2\pi\tau T)} + \frac{2\cos(2\pi\tau T)}{\sin^2(2\pi\tau T)} + \frac{1}{6}\right]\,. \tag{5.13}$$

The results are shown in figure 4, and indicate good overall agreement.

5.3 On soft corrections

In order to be more precise than eq. (5.12), NLO *thermal* corrections to $\rho_{\rm T}$, $\rho_{\rm L}$ are needed for $|\mathcal{K}^2| \gtrsim (\pi T)^2$ and, perhaps more importantly, the soft domain $|\mathcal{K}^2| \ll (\pi T)^2$ needs to be properly addressed. If the correlators G_{00}, G_{11}, G_{22+33} are inspected separately, we may expect qualitatively different corrections from the soft domain than for the vector channel correlator $G_{00} - G_{ii}$. One way to see this is that at LO both the spectral function $\{\mathrm{Im}\,\Pi_{\rm R}\}_{00} = -k^2\,\rho_{\rm L}/\mathcal{K}^2$ and $\{\mathrm{Im}\,\Pi_{\rm R}\}_{11} = -k_0^2\,\rho_{\rm L}/\mathcal{K}^2$ are discontinuous across $k_0 = k$,

JHEP11(2013)120

whereas their difference $\{\mathrm{Im}\,\Pi_{\mathrm{R}}\}_{00} - \{\mathrm{Im}\,\Pi_{\mathrm{R}}\}_{11} = \rho_{\mathrm{L}}$ is continuous and vanishes for $k_0 = k$, as is the case also with $\{\mathrm{Im}\,\Pi_{\mathrm{R}}\}_{22} = \{\mathrm{Im}\,\Pi_{\mathrm{R}}\}_{33} = -\rho_{\mathrm{T}}$. Therefore at LO the light-cone regime makes a smaller contribution to $G_{00} - G_{ii}$ than to G_{00} and G_{11}. On the other hand, after accounting for thermal loop corrections, ρ_{T} no longer vanishes at the light-cone, so NLO corrections may be relatively speaking larger in G_{22+33} than in G_{00} and G_{11}. Indeed, it can be observed in figure 4 that there is a larger discrepancy in G_{22+33} than in G_{11}.

For $k = 0$, in which case there are no ambiguities (there is no contribution from $k_0 < k$ and G_{00} is a known constant), the discrepancy between lattice data and the perturbative correlator is small. Yet it was found in ref. [20] that the discrepancy can be used for constraining the parameters of a transport peak, such as the diffusion coefficient D, in a non-trivial way. It will be interesting to see how large a discrepancy remains there for $k \neq 0$ in a continuum-extrapolated $G_{00} - G_{ii}$ and whether it can be accounted for by the physics of the soft regime in a similar way. As a first step strict NLO expressions, i.e. results from the current paper supplemented by a similar analysis at $k_0 < k$, may be used; the logarithmic divergence they contain at $\mathcal{K}^2 = 0$ is integrable. Going beyond this, LPM-resummed results could be tested, however for the moment none seem to exist for $k_0 < k$. The range $k_0 < k$ has been studied in a leading-logarithmic approximation in ref. [43] and within a holographic framework in ref. [44], in both cases even for ρ_{T} and ρ_{L} separately. For $k_0, k \to 0$, ρ_{T} and ρ_{L} can also be parametrised by D and second order transport coefficients, cf. e.g. ref. [43]. (A general discussion of various domains can be found, for $k = 0$, in ref. [45].)

6 Conclusions

The purpose of this paper has been to determine the vector channel spectral function (cf. figure 1) and the dilepton production rate (cf. figure 3) up to next-to-leading order in thermal QCD, keeping track of a non-zero momentum of the dilepton pair with respect to the heat bath. The results are reliable in a characteristically "thermal" regime, $\mathcal{K}^2 \gtrsim (\pi T)^2$, which for heavy ion collision experiments corresponds to $\mathcal{K}^2 \gtrsim 1\ \mathrm{GeV}^2$.

In the regime considered, the expressions obtained are complicated enough that no analytic representations have been found for all the structures appearing; we have rather evaluated 2-dimensional integrals numerically for the different "basis functions" needed (cf. figure 5). However, in a "hard" limit $\mathcal{K}^2 \gg (\pi T)^2$ an explicit expression, given in eq. (3.5), can be obtained [7]. By comparing with the numerical evaluation of figure 1, the asymptotic form of eq. (3.5) is seen to be accurate in the range $\mathcal{K}^2 \gtrsim (8T)^2$ (cf. figure 2).

In the opposite regime $0 < \mathcal{K}^2 \ll (\pi T)^2$, the naive loop expansion breaks down and resummations are needed for obtaining formally consistent results. We have observed, however, that as long as $\ln\{(\pi T)^2/\mathcal{K}^2\}$ is not large, even the naive results of the present paper agree relatively well with resummed ones [12]. The explanation could be that the resummation is numerically not overwhelmingly important for moderate $\mathcal{K}^2 \sim (gT)^2$; those parts of it already included in the current expression, together with all "hard" processes such as $2 \leftrightarrow 2$ scatterings, may capture much of the answer. (Resummation is also tricky in that it is non-trivial to avoid double counting when the resummed result is combined with hard processes [13].)

JHEP11(2013)120

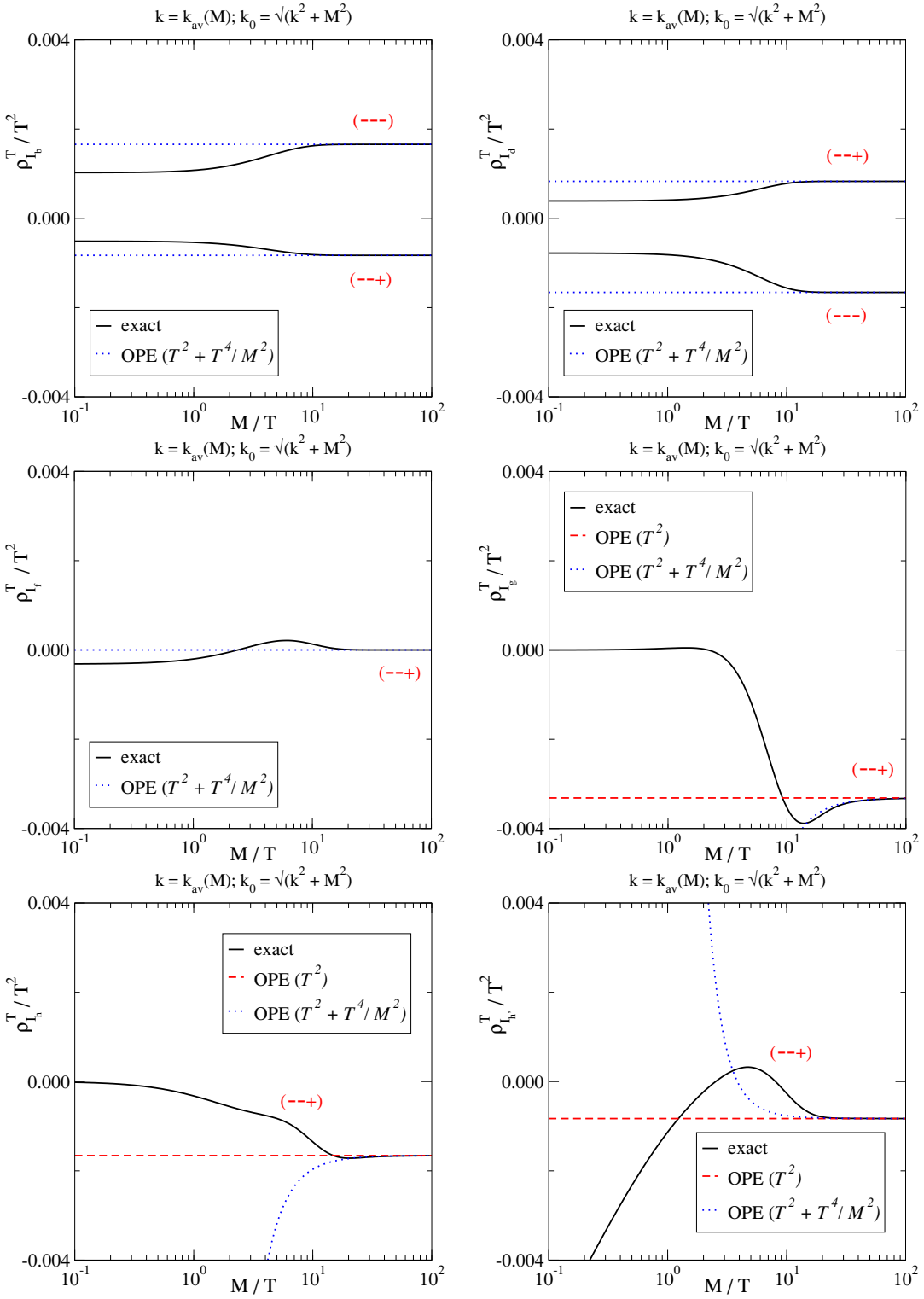

Figure 5. Thermal parts of spectral functions corresponding to eqs. (A.2)–(A.9), with spatial momentum fixed according to eq. (A.12). The indices refer to $(\sigma_1\sigma_4\sigma_5)$, cf. eqs. (2.12), (2.13).

JHEP11(2013)120

In the regime $\mathcal{K}^2 \gtrsim (1\,\mathrm{GeV})^2$, the uncertainties of the current results could be on a 10–30% level, judging from the scale dependence in figure 3. For a comparison with actual data, the results should be embedded in a hydrodynamical model incorporating the temperature evolution of the system, which unfortunately goes beyond the scope of the present study.

Apart from heavy ion data, we have elaborated on possibilities to confront spectral functions with continuum-extrapolated lattice results (cf. figure 4). This comparison is ambiguous for the moment, given that continuum-extrapolated data are only available for spatial components of the vector correlator and that also the domain below the light-cone ($\mathcal{K}^2 < 0$) contributes to imaginary-time correlators measured on the lattice. Once these issues have been addressed, it appears that accounting for the difference of a "hard" perturbative contribution and a continuum-extrapolated lattice correlator may permit for a non-trivial crosscheck of the physics of the soft domain. Apart from soft dilepton spectra, this might give another handle on the diffusion coefficient D, complementing its direct estimate as a transport coefficient from measurements at $k = 0$.

Acknowledgments

I am grateful to A. Francis for providing numerical data from ref. [19] and for helpful discussions, and to H.B. Meyer and G.D. Moore for helpful discussions. This work was partly supported by the Swiss National Science Foundation (SNF) under grant 200021-140234.

A Definitions of master sum-integrals

Denoting by $\sum\!\!\!\!\!\!\int_P$ and $\sum\!\!\!\!\!\!\int_{\{P\}}$ sum-integrals over bosonic and fermionic Matsubara four-momenta, the master sum-integrals yielding non-vanishing cuts are defined as follows (a dashed line indicates a bosonic propagator, a solid line a fermionic one, a filled blob a squared propagator, and a cross a structure in the numerator):

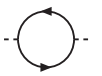

$$\mathcal{J}_{\mathrm{b}} \equiv \sum\!\!\!\!\!\!\int_{\{P\}} \frac{K^2}{P^2(P-K)^2} \,, \tag{A.1}$$

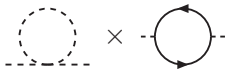

$$\bar{\bar{\mathcal{I}}}_{\mathrm{b}} \equiv \sum\!\!\!\!\!\!\int_{\{P\}Q} \frac{1}{Q^2P^2(P-K)^2} \,, \tag{A.2}$$

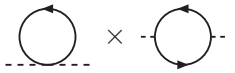

$$\mathcal{I}_{\mathrm{b}} \equiv \sum\!\!\!\!\!\!\int_{\{PQ\}} \frac{1}{Q^2P^2(P-K)^2} \,, \tag{A.3}$$

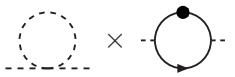

$$\bar{\bar{\mathcal{I}}}_{\mathrm{d}} \equiv \sum\!\!\!\!\!\!\int_{\{P\}Q} \frac{K^2}{Q^2P^4(P-K)^2} \,, \tag{A.4}$$

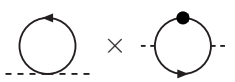

$$\mathcal{I}_{\mathrm{d}} \equiv \sum\!\!\!\!\!\!\int_{\{PQ\}} \frac{K^2}{Q^2P^4(P-K)^2} \,, \tag{A.5}$$

$$\mathcal{I}_{\mathrm{f}} \equiv \lim_{\lambda\to 0} \sum\!\!\!\!\!\!\int_{\{PQ\}} \frac{1}{Q^2[(Q-P)^2+\lambda^2](P-K)^2} \,, \tag{A.6}$$

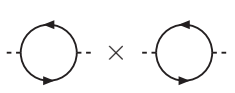

$$\mathcal{I}_{\mathrm{g}} \equiv \sum\!\!\!\!\!\!\int_{\{PQ\}} \frac{K^2}{P^2(P-K)^2Q^2(Q-K)^2} \,, \tag{A.7}$$

$$\mathcal{I}_{\rm h} \equiv \lim_{\lambda\to 0} \sum\!\!\!\!\!\!\int_{\{PQ\}} \frac{K^2}{Q^2P^2[(Q-P)^2+\lambda^2](P-K)^2} \,, \tag{A.8}$$

$$\mathcal{I}_{\rm h'} \equiv \lim_{\lambda\to 0} \sum\!\!\!\!\!\!\int_{\{PQ\}} \frac{2K\cdot Q}{Q^2P^2[(Q-P)^2+\lambda^2](P-K)^2} \,, \tag{A.9}$$

$$\mathcal{I}_{\rm j} \equiv \lim_{\lambda\to 0} \sum\!\!\!\!\!\!\int_{\{PQ\}} \frac{K^4}{Q^2P^2[(Q-P)^2+\lambda^2](P-K)^2(Q-K)^2} \,, \tag{A.10}$$

a generic labelling of the lines is employed (with individual propagators omitted for the simpler masters):

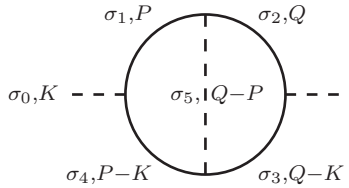

. (A.11)

The labels $\sigma_0,\ldots,\sigma_5$ take the value $+1$ for bosons and -1 for fermions. The expressions for the corresponding spectral functions have been worked out in refs. [23, 24], and we refer to these works for more details. Numerical results are shown in figure 5, except for the case $\mathcal{I}_{\rm j}$ for which numerical results were already shown in ref. [23]. The average momentum employed in figure 5 is defined as

$$k^2_{\rm av}(M) \equiv \frac{\int_0^\infty {\rm d}k\, k^4 \exp\left(-\frac{\sqrt{k^2+M^2}}{T}\right)}{\int_0^\infty {\rm d}k\, k^2 \exp\left(-\frac{\sqrt{k^2+M^2}}{T}\right)} = \frac{3MTK_3\left(\frac{M}{T}\right)}{K_2\left(\frac{M}{T}\right)} \,. \tag{A.12}$$

B Choice of parameters

The strong coupling constant runs as $\partial_t a_s = -\left(\beta_0 a_s^2 + \beta_1 a_s^3 + \beta_2 a_s^4 + \beta_3 a_s^5 + \ldots\right)$, where $a_s \equiv \alpha_s(\bar\mu)/\pi$, $t \equiv \ln\left(\bar\mu^2/\Lambda^2_{\overline{\rm MS}}\right)$, and, for $N_{\rm c} = 3$ [46],

$$\beta_0 = \frac{11}{4} - \frac{N_{\rm f}}{6} \,, \qquad \beta_1 = \frac{51}{8} - \frac{19N_{\rm f}}{24} \,, \qquad \beta_2 = \frac{2857}{128} - \frac{5033N_{\rm f}}{1152} + \frac{325N_{\rm f}^2}{3456} \,, \tag{B.1}$$

$$\beta_3 = \frac{149753 + 21384\zeta(3)}{1536} - \frac{[1078361 + 39048\zeta(3)]N_{\rm f}}{41472} + \frac{[50065 + 12944\zeta(3)]N_{\rm f}^2}{41472} + \frac{1093N_{\rm f}^3}{186624} \,. \tag{B.2}$$

The scale parameter $\Lambda_{\overline{\rm MS}}$ represents an integration constant and is chosen so that the asymptotic ($t \gg 1$) behaviour reads

$$a_s = \frac{1}{\beta_0 t} - \frac{\beta_1 \ln t}{\beta_0^3 t^2} + \frac{\beta_1^2\left(\ln^2 t - \ln t - 1\right) + \beta_2\beta_0}{\beta_0^5 t^3} + \mathcal{O}\left(\frac{1}{t^4}\right) \,. \tag{B.3}$$

The renormalization scale is varied within the range

$$\bar\mu \in (0.5\ldots 2.0)\,\bar\mu_{\rm ref} \,, \qquad \bar\mu^2_{\rm ref} \equiv \max\left\{\mathcal{K}^2, (\pi T)^2\right\} \,. \tag{B.4}$$

In general we have employed 3-loop running (i.e. $\beta_0, \beta_1, \beta_2$) given that this corresponds to the formal accuracy of eq. (5.11), however we have checked that results obtained with 4-loop running are well within the error band obtained from eq. (B.4).

JHEP11(2013)120

References

[1] M. Le Bellac, *Thermal Field Theory*, Cambridge University Press, Cambridge, (2000).

[2] J.I. Kapusta and C. Gale, *Finite-Temperature Field Theory: Principles and Applications*, Cambridge University Press, Cambridge, (2006).

[3] R. Baier, B. Pire and D. Schiff, *Dilepton production at finite temperature: Perturbative treatment at order α_s*, *Phys. Rev.* **D 38** (1988) 2814 [INSPIRE].

[4] Y. Gabellini, T. Grandou and D. Poizat, *Electron-Positron Annihilation in Thermal QCD*, *Annals Phys.* **202** (1990) 436 [INSPIRE].

[5] T. Altherr and P. Aurenche, *Finite temperature QCD corrections to lepton pair formation in a quark-gluon plasma*, *Z. Phys.* **C 45** (1989) 99 [INSPIRE].

[6] Y. Burnier, M. Laine and M. Vepsäläinen, *Heavy quark medium polarization at next-to-leading order*, *JHEP* **02** (2009) 008 [arXiv:0812.2105] [INSPIRE].

[7] S. Caron-Huot, *Asymptotics of thermal spectral functions*, *Phys. Rev.* **D 79** (2009) 125009 [arXiv:0903.3958] [INSPIRE].

[8] P.A. Baikov, K.G. Chetyrkin and J.H. Kühn, *Order α_s^4 QCD Corrections to Z and τ Decays*, *Phys. Rev. Lett.* **101** (2008) 012002 [arXiv:0801.1821] [INSPIRE].

[9] P.A. Baikov, K.G. Chetyrkin, J.H. Kühn and J. Rittinger, *Adler Function, Sum Rules and Crewther Relation of Order $O(\alpha_s^4)$: the Singlet Case*, *Phys. Lett.* **B 714** (2012) 62 [arXiv:1206.1288] [INSPIRE].

[10] E. Braaten, R.D. Pisarski and T.-C. Yuan, *Production of Soft Dileptons in the quark-gluon Plasma*, *Phys. Rev. Lett.* **64** (1990) 2242 [INSPIRE].

[11] D. Besak and D. Bödeker, *Hard Thermal Loops for Soft or Collinear External Momenta*, *JHEP* **05** (2010) 007 [arXiv:1002.0022] [INSPIRE].

[12] P. Aurenche, F. Gelis, G.D. Moore and H. Zaraket, *Landau-Pomeranchuk-Migdal resummation for dilepton production*, *JHEP* **12** (2002) 006 [hep-ph/0211036] [INSPIRE].

[13] M.E. Carrington, A. Gynther and P. Aurenche, *Energetic di-leptons from the Quark Gluon Plasma*, *Phys. Rev.* **D 77** (2008) 045035 [arXiv:0711.3943] [INSPIRE].

[14] G.D. Moore and J.-M. Robert, *Dileptons, spectral weights and conductivity in the quark-gluon plasma*, hep-ph/0607172 [INSPIRE].

[15] P.B. Arnold, G.D. Moore and L.G. Yaffe, *Photon emission from ultrarelativistic plasmas*, *JHEP* **11** (2001) 057 [hep-ph/0109064] [INSPIRE].

[16] P.B. Arnold, G.D. Moore and L.G. Yaffe, *Photon emission from quark gluon plasma: Complete leading order results*, *JHEP* **12** (2001) 009 [hep-ph/0111107] [INSPIRE].

[17] P.B. Arnold, G.D. Moore and L.G. Yaffe, *Photon and gluon emission in relativistic plasmas*, *JHEP* **06** (2002) 030 [hep-ph/0204343] [INSPIRE].

[18] H.-T. Ding, A. Francis, O. Kaczmarek, F. Karsch, E. Laermann and W. Soeldner, *Thermal dilepton rate and electrical conductivity: An analysis of vector current correlation functions in quenched lattice QCD*, *Phys. Rev.* **D 83** (2011) 034504 [arXiv:1012.4963] [INSPIRE].

[19] H.-T. Ding et al., *Thermal dilepton rates from quenched lattice QCD*, PoS(Confinement X)185 [arXiv:1301.7436] [INSPIRE].

JHEP11(2013)120

[20] Y. Burnier and M. Laine, *Towards flavour diffusion coefficient and electrical conductivity without ultraviolet contamination*, *Eur. Phys. J.* **C 72** (2012) 1902 [arXiv:1201.1994] [INSPIRE].

[21] B.B. Brandt, A. Francis, H.B. Meyer and H. Wittig, *Thermal correlators in the ρ channel of two-flavor QCD*, *JHEP* **03** (2013) 100 [arXiv:1212.4200] [INSPIRE].

[22] A. Amato, G. Aarts, C. Allton, P. Giudice, S. Hands and J.-I. Skullerud, *Electrical conductivity of the quark-gluon plasma across the deconfinement transition*, *Phys. Rev. Lett.* **111** (2013) 172001 [arXiv:1307.6763] [INSPIRE].

[23] M. Laine, *Thermal 2-loop master spectral function at finite momentum*, *JHEP* **05** (2013) 083 [arXiv:1304.0202] [INSPIRE].

[24] M. Laine, *Thermal right-handed neutrino production rate in the relativistic regime*, *JHEP* **08** (2013) 138 [arXiv:1307.4909] [INSPIRE].

[25] L.D. McLerran and T. Toimela, *Photon and dilepton emission from the quark-gluon plasma: Some general considerations*, *Phys. Rev.* **D 31** (1985) 545 [INSPIRE].

[26] H.A. Weldon, *Reformulation of finite temperature dilepton production*, *Phys. Rev.* **D 42** (1990) 2384 [INSPIRE].

[27] C. Gale and J.I. Kapusta, *Vector dominance model at finite temperature*, *Nucl. Phys.* **B 357** (1991) 65 [INSPIRE].

[28] M. Laine, A. Vuorinen and Y. Zhu, *Next-to-leading order thermal spectral functions in the perturbative domain*, *JHEP* **09** (2011) 084 [arXiv:1108.1259] [INSPIRE].

[29] Y. Zhu and A. Vuorinen, *The shear channel spectral function in hot Yang-Mills theory*, *JHEP* **03** (2013) 002 [arXiv:1212.3818] [INSPIRE].

[30] M. Laine, M. Vepsäläinen and A. Vuorinen, *Ultraviolet asymptotics of scalar and pseudoscalar correlators in hot Yang-Mills theory*, *JHEP* **10** (2010) 010 [arXiv:1008.3263] [INSPIRE].

[31] Y. Schröder, M. Vepsäläinen, A. Vuorinen and Y. Zhu, *The ultraviolet limit and sum rule for the shear correlator in hot Yang-Mills theory*, *JHEP* **12** (2011) 035 [arXiv:1109.6548] [INSPIRE].

[32] M. Laine and Y. Schröder, *Thermal right-handed neutrino production rate in the non-relativistic regime*, *JHEP* **02** (2012) 068 [arXiv:1112.1205] [INSPIRE].

[33] H.A. Weldon, *Effective Fermion Masses of Order gT in High Temperature Gauge Theories with Exact Chiral Invariance*, *Phys. Rev.* **D 26** (1982) 2789 [INSPIRE].

[34] G. Aarts and J.M. Martínez Resco, *Continuum and lattice meson spectral functions at nonzero momentum and high temperature*, *Nucl. Phys.* **B 726** (2005) 93 [hep-lat/0507004] [INSPIRE].

[35] T. Altherr and P. Ruuskanen, *Low mass dileptons at high momenta in ultrarelativistic heavy ion collisions*, *Nucl. Phys.* **B 380** (1992) 377 [INSPIRE].

[36] H.A. Weldon, *Simple rules for discontinuities in finite-temperature field theory*, *Phys. Rev.* **D 28** (1983) 2007 [INSPIRE].

[37] J.I. Kapusta, P. Lichard and D. Seibert, *High-energy photons from quark-gluon plasma versus hot hadronic gas*, *Phys. Rev.* **D 44** (1991) 2774 [*Erratum ibid.* **D 47** (1993) 4171] [INSPIRE].

JHEP11(2013)120

[38] R. Baier, H. Nakkagawa, A. Niégawa and K. Redlich, *Production rate of hard thermal photons and screening of quark mass singularity*, *Z. Phys.* **C 53** (1992) 433 [INSPIRE].

[39] PACS-CS collaboration, S. Aoki et al., *Precise determination of the strong coupling constant in $N_f = 2 + 1$ lattice QCD with the Schrödinger functional scheme*, *JHEP* **10** (2009) 053 [arXiv:0906.3906] [INSPIRE].

[40] Y. Burnier, M. Laine and L. Mether, *A test on analytic continuation of thermal imaginary-time data*, *Eur. Phys. J.* **C 71** (2011) 1619 [arXiv:1101.5534] [INSPIRE].

[41] G. Cuniberti, E. De Micheli and G.A. Viano, *Reconstructing the thermal Green functions at real times from those at imaginary times*, *Commun. Math. Phys.* **216** (2001) 59 [cond-mat/0109175] [INSPIRE].

[42] W. Florkowski and B.L. Friman, *Spatial dependence of the finite temperature meson correlation function*, *Z. Phys.* **A 347** (1994) 271 [INSPIRE].

[43] J. Hong and D. Teaney, *Spectral densities for hot QCD plasmas in a leading log approximation*, *Phys. Rev.* **C 82** (2010) 044908 [arXiv:1003.0699] [INSPIRE].

[44] S. Caron-Huot, P. Kovtun, G.D. Moore, A. Starinets and L.G. Yaffe, *Photon and dilepton production in supersymmetric Yang-Mills plasma*, *JHEP* **12** (2006) 015 [hep-th/0607237] [INSPIRE].

[45] P.B. Arnold and L.G. Yaffe, *Effective theories for real time correlations in hot plasmas*, *Phys. Rev.* **D 57** (1998) 1178 [hep-ph/9709449] [INSPIRE].

[46] T. van Ritbergen, J.A.M. Vermaseren and S.A. Larin, *The four loop β-function in Quantum Chromodynamics*, *Phys. Lett.* **B 400** (1997) 379 [hep-ph/9701390] [INSPIRE].

JHEP11(2013)120